

Methyl Group-Induced Helicity in 1,4-Dimethylbenzo[*c*]phenanthrene and Its Metabolites: Synthesis, Physical, and Biological Properties

Mahesh K. Lakshman,^{*,†,‡,§} Panna L. Kole,[‡] Surendrakumar Chaturvedi,^{‡,||} Joseph H. Saugier,[‡] Herman J. C. Yeh,^{*,⊥} Jenny P. Glusker,^{*,#} H. L. Carrell,[#] Amy K. Katz,[#] Carol E. Afshar,[#] Won-Mohaiza Dashwood,[§] Gary Kenniston,[§] and William M. Baird^{*,§,&}

Contribution from the Department of Chemistry, University of North Dakota, Grand Forks, North Dakota 58202, Chemsyn Science Laboratories, 13605 West 96th Terrace, Lenexa, Kansas 66215, PE Biosystems, 850 Lincoln Center Drive, Foster City, California 94404, LBC, NIDDK, National Institutes of Health, Bethesda, Maryland 20892, The Institute for Cancer Research, Fox Chase Cancer Center, 7701 Burholme Avenue, Philadelphia, Pennsylvania 19111, Environmental and Molecular Toxicology, Oregon State University, Corvallis, Oregon 97331, and Environmental Health Sciences Center, Oregon State University, Corvallis, Oregon 97331

Received June 9, 2000

Abstract: 1,4-Dimethylbenzo[*c*]phenanthrene (1,4-DMBcPh) is the dimethylated analogue of the benzo[*c*]phenanthrene (BcPh), where one of its two methyl groups resides in the highly congested fjord-region. A comparative X-ray crystallographic analysis, described herein, shows that BcPh is distorted out-of-plane so that there is an angle of 27° between the outermost rings. The additional methyl groups in 1,4-DMBcPh increase this nonplanarity to an angle of 37°. This methyl group-induced disruption of planarity results in *P* and *M* enantiomers of 1,4-DMBcPh, and this helicity is observed in a pronounced manner in its putative metabolites, the dihydrodiol and diol epoxide. Synthetically, photochemical cyclization offers convenient access to 1,4-DMBcPh as well as its metabolites. For this, Wittig reaction of 2,5-dimethylbenzyltriphenylphosphonium chloride and 2-naphthaldehyde provided a *cis/trans* mixture of alkenes which, when subjected to photolysis, provided 1,4-DMBcPh. Despite the high steric congestion in the fjord-region, this reaction proceeds with respectable yields. Correspondingly, a Wittig reaction of the same phosphonium chloride derivative with 6-methoxy-2-naphthaldehyde afforded an alkene mixture that, upon photochemical ring closure, provided 10-methoxy-1,4-dimethylbenzo[*c*]phenanthrene. The methoxy group was cleaved and the resulting phenol oxidized to the *o*-quinone. Reduction of the *o*-quinone with NaBH₄ under an oxygen atmosphere provided the dihydrodiol, (±)-*trans*-9,10-dihydroxy-9,10-dihydro-1,4-dimethylbenzo[*c*]phenanthrene. This dihydrodiol was found to be an approximately 3:1 mixture of diastereomers, which was produced as follows. Reduction of the quinone proceeds in a stereoselective manner producing both the (*R,R*)- and (*S,S*)-*trans*-diols. However, this factor, when coupled with the *P*, *M* atropisomerism of the hydrocarbon, results in two diastereomeric pairs of enantiomeric dihydrodiols. Due to steric constraints imposed by the fjord-region methyl group, the *P* → *M* interconversion is slow, making the proton resonances of the diastereomeric dihydrodiols distinctly observable by NMR. Assignment of major and minor dihydrodiol isomers has been achieved by NOESY experiments. Finally, epoxidation provides a mixture of diol epoxides that reflects the dihydrodiol ratio. The metabolic activation of these compounds to reactive intermediates was studied through analysis of their binding to DNA. DNA binding data using human mammary carcinoma MCF-7 cells reveal that the level of DNA binding of BcPh is not statistically different from that of 1,4-DMBcPh. However, there is an 11-fold increased activation of BcPh dihydrodiol as compared to the 1,4-DMBcPh dihydrodiol. In contrast to the planar benzo[*a*]pyrene, BcPh is only poorly adducted to DNA in culture cells. Thus, it appears that increasing the nonplanarity in this type of PAH lowers its ability to be metabolically activated to form DNA-damaging adducts, although in the case of 1,4-DMBcPh, the presence of the two methyl groups in one of the angular rings may also contribute to the decrease.

Introduction

The high environmental prevalence of polycyclic aromatic hydrocarbons (PAHs) and the cancer threat these compounds

* Corresponding authors: Please address inquiries about the synthesis to M.K.L., X-ray crystallography to J.P.G., metabolism studies to W.M.B., and NMR studies to H.J.C.Y.

† University of North Dakota.

‡ Chemsyn Science Laboratories.

§ Present address: Department of Chemistry, City College of CUNY, 138th St. and Convent Ave., New York, NY 10031; (e-mail) lakshman@sci.ccny.cuny.edu.

|| PE Biosystems.

⊥ National Institutes of Health.

The Institute for Cancer Research.

§ Environmental and Molecular Toxicology, Oregon State University.

& Environmental Health Sciences Center, Oregon State University.

pose to humans, has drawn substantial attention to these compounds.¹ Specifically, the metabolism and mode of action of PAHs containing a bay or fjord-region has attracted the interest of investigators.² Benzo[*c*]phenanthrene (BcPh, **1**; see Figure 1) is the prototype for PAHs that contain a highly congested fjord-region, and this congestion leads to substantial nonplanarity of the compound. BcPh is a weak carcinogen in

(1) PAH carcinogenesis has been reviewed in: *Polycyclic Aromatic Hydrocarbon Carcinogenesis: Structure–Activity Relationships*; Yang, S. K., Silverman, B. D., Eds.; CRC Press: Boca Raton, FL, 1988; Vols. I and II. *Polycyclic Aromatic Hydrocarbons: Chemistry and Carcinogenicity*; Harvey, R. G., Ed.; Cambridge University Press: Cambridge, 1991. *Polycyclic Hydrocarbons and Carcinogenesis*; Harvey, R. G., Ed.; ACS Symposium Series 283: American Chemical Society: Washington, DC, 1985.

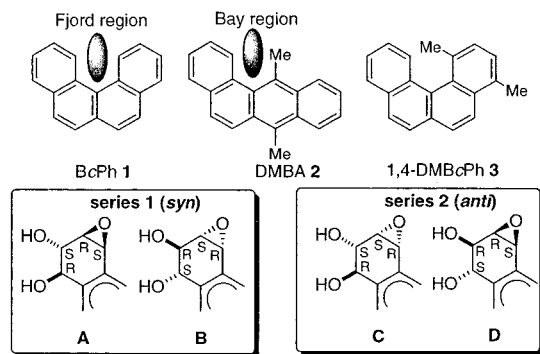


Figure 1. Structures of the highly hindered PAHs: benzo[*c*]phenanthrene (**1**), 7,12-dimethylbenzo[*a*]anthracene (**2**), and 1,4-dimethylbenzo[*c*]phenanthrene (**3**) as well as partial structures of the four isomeric, angular ring diol epoxide metabolites.

the mouse skin model and is metabolized to a minor extent to angular ring diol epoxides.³ The fjord-region diol epoxide metabolites of BcPh have rather interesting properties compared to the less congested bay-region analogues. For instance, the fjord-region diol epoxides of BcPh are the most potent DNA alkylating agents among this class of compounds,⁴ and the (4*R*,3*S*)-diol (2*S*,1*R*)-epoxide isomer (Figure 1, **C**) is the most tumorigenic diol epoxide synthesized to date.⁵ Additionally, the series 1 (syn) diol epoxides of BcPh exhibit a quasi-diequatorial arrangement of hydroxyl groups, a feature not normally associated with these isomers.^{3,6} Another unusual factor, which is possibly related to the hydroxyl group orientation, is the high tumorigenic activity of the (4*S*,3*R*)-diol (2*S*,1*R*)-epoxide (Figure 1, **B**), which is unprecedented among similar metabolites of hydrocarbons containing a bay-region.⁷

In contrast to the diol epoxides of the planar PAHs (such as benzo[*a*]pyrene (BaP), chrysene, and benzo[*a*]anthracene), which preponderantly alkylate the *N*²-amino group of deoxyguanosine residues in reactions with DNA in its minor groove,⁸ the diol epoxides of BcPh show significantly higher alkylation of the *N*⁶-amino group of deoxyadenosine residues in the major groove of DNA.^{8,9} Studies with the nonplanar series 2 (anti) diol epoxides of the potent carcinogens 7,12-dimethylbenzo[*a*]anthracene (DMBA, **2**, Figure 1)¹⁰ and benzo[*g*]chrysene

(BgCh)¹¹ also show similar increased alkylation at deoxyadenosine in DNA binding reactions. Thus, bulky nonplanar PAH metabolites are more likely to bind in these less hindered areas of DNA. These observations have led to the question of whether hydrocarbon nonplanarity plays a role in the site of DNA alkylation and the overall effect of increased deoxyadenosine alkylation on the tumorigenicities of PAHs.¹²

The influence of planarity (or lack thereof) on the metabolic activation and DNA binding properties of PAHs forms the basis of this article. Controlled introduction of substituents into a PAH nucleus can be used to produce the desired distortions in the PAH and the extent of nonplanarity in the resulting compounds can be readily ascertained by X-ray crystallographic studies. A comparison of the metabolic activation and DNA binding data of these PAHs and their metabolites with known data could then lead to a better understanding of the role of nonplanarity in the biological outcome.

1,4-Dimethylbenzo[*c*]phenanthrene (1,4-DMBcPh, **3**, Figure 1) is an attractive starting point for several reasons: (a) the metabolism of BcPh and DNA binding properties of its diol epoxides are known, (b) 1,4-DMBcPh is isomeric with the potent carcinogen DMBA, and just as the bay-region methyl produces distortion in the DMBA nucleus, the fjord-region methyl should increase the nonplanarity of BcPh, (c) syntheses of 1,4-DMBcPh and its derivatives are apparently simpler than those of fjord-region monomethyl BcPh, and (d) dihydrodiols and diol epoxides of methylated fjord-region containing PAHs have not been reported to date.

In this study, we describe convenient synthetic routes to 1,4-DMBcPh, its (±)-trans 9,10-dihydrodiol as well as the (±)-9β,10α-diol 11α,12α-epoxide. Comparative metabolic activation and DNA binding of BcPh, 1,4-DMBcPh, and their dihydrodiols has also been investigated using mammary carcinoma MCF-7 cells. During the course of this synthesis, we show that a fjord-region methyl can induce helicity in this small hydrocarbon which then results in the hydrocarbon demonstrating atropisomerism (*P* and *M* helicity). X-ray crystallographic analyses of BcPh and 1,4-DMBcPh were undertaken in order to evaluate the extent of distortion caused by the methyl group.

Results and Discussion

Synthesis of 1,4-DMBcPh and Its Dihydrodiol. Photochemical ring closure of appropriate stilbenes to phenanthrenes has proven to be a good method for the synthesis of several angular ring-fused PAHs,¹³ and extensions of this method for the synthesis of fjord-region dihydrodiols have been documented.¹⁴ However, for the present study, the suitability of this method was not known since the introduction of a fjord-region methyl group on the course of the photocyclization had not been

(2) Reviewed in: Thakker, D. R.; Levin, W.; Wood, A. W.; Conney, A. H.; Yagi, H.; Jerina, D. M. In *Drug Stereochemistry, Analytical Methods and Pharmacology*; Wainer, I. W., Drayer, D. E., Eds.; Marcel Dekker: New York, 1988; pp 271–296. Jerina, D. M.; Sayer, J. M.; Agarwal, S. K.; Yagi, H.; Levin, W.; Wood, A. W.; Conney, A. H.; Pruess-Schwartz, D.; Baird, W. M.; Pigott, M. A.; Dipple, A. In *Biological Reactive Intermediates III*; Kocsis, J. J., Jollow, D. J., Witmer, C. M., Nelson, J. O., Snyder, R., Eds.; Plenum Press: New York, 1986; pp 11–30.

(3) Jerina, D. M.; Sayer, J. M.; Yagi, H.; Croisy-Delcey, M.; Ittah, Y.; Thakker, D. R.; Wood, A. W.; Chang, R. L.; Levin, W.; Conney, A. H. In *Biological Reactive Intermediates II Part A*; Snyder, R., Parke, D. V., Kocsis, J. J., Jollow, D. J., Gibson, C. G., Witmer, C. M., Eds.; Plenum Press: New York, 1986; pp 501–523.

(4) Agarwal, S. K.; Sayer, J. M.; Yeh, H. J. C.; Pannell, L. K.; Hilton, B. D.; Pigott, M. A.; Dipple, A.; Yagi, H.; Jerina, D. M. *J. Am. Chem. Soc.* **1987**, *109*, 2497–2504.

(5) Jerina, D. M.; Chadha, A.; Cheh, A. M.; Schurdak, M. E.; Wood, A. W.; Sayer, J. M. In *Biological Reactive Intermediates IV*; Witmer, C. M., Snyder, R., Jollow, D. J., Kalf, G. F., Kocsis, J. J., Sipes, I. G., Eds.; Plenum Press: New York, 1991; pp 533–553.

(6) Sayer, J. M.; Yagi, H.; Croisy-Delcey, M.; Jerina, D. M. *J. Am. Chem. Soc.* **1981**, *103*, 4970–4972.

(7) Levin, W.; Chang, R. L.; Wood, A. W.; Thakker, D. R.; Yagi, H.; Jerina, D. M.; Conney, A. H. *Cancer Res.* **1986**, *46*, 2257–2261.

(8) Dipple, A. In *DNA Adducts: Identification and Biological Significance*; Hemminki, K., Dipple, A., Shuker, D. E. G., Kadlubar, F. F., Sagerbäck, D., Bartsch, H., Eds.; Scientific Publication No. 125; International Agency for Research on Cancer: Lyon, 1994; pp 107–129.

(9) Dipple, A.; Pigott, M. A.; Agarwal, S. K.; Yagi, H.; Sayer, J. M.; Jerina, D. M. *Nature* **1987**, *327*, 535–536.

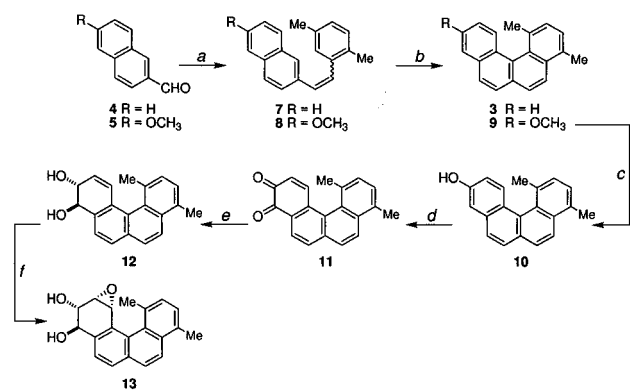
(10) Cheng, S. C.; Prakash, A. S.; Pigott, M. A.; Hilton, B. D.; Lee, H.; Harvey, R. G.; Dipple, A. *Carcinogenesis* **1988**, *9*, 1721–1723.

(11) Szeliga, J.; Lee, H.; Harvey, R. G.; Page, J. E.; Ross, H. L.; Routledge, M. N.; Hilton, B. D.; Dipple, A. *Chem. Res. Toxicol.* **1994**, *7*, 420–427. Szeliga, J.; Page, J. E.; Hilton, B. D.; Kiselyov, A. S.; Harvey, R. G.; Dunayevskiy, Y. M.; Vouros, P.; Dipple, A. *Chem. Res. Toxicol.* **1995**, *8*, 1014–1019.

(12) Szeliga, J.; Dipple, A. *Chem. Res. Toxicol.* **1998**, *11*, 1–11.

(13) Caruthers, W. *J. Chem. Soc.* **1967**, 1525–1527. Mallory, F. B.; Rudolph, M. J.; Oh, S. M. *J. Org. Chem.* **1989**, *54*, 4619–4626 and references therein.

(14) (a) Amin, S.; Camanzo, J.; Huie, K.; Hecht, S. S. *J. Org. Chem.* **1984**, *49*, 381–384. (b) Utermohlen, C. M.; Singh, M.; Lehr, R. E. *J. Org. Chem.* **1987**, *52*, 5574–5582. (c) Amin, S.; Balanikas, G.; Huie, K.; Hecht, S. S. *Chem. Res. Toxicol.* **1988**, *1*, 349–355. (d) Misra, B.; Amin, S. *J. Org. Chem.* **1990**, *55*, 4478–4480. (e) Krzeminski, J.; Lin, J.-M.; Amin, S.; Hecht, S. S. *Chem. Res. Toxicol.* **1994**, *7*, 125–129. (f) Seidel, A.; Luch, A.; Platt, K. L.; Oesch, F.; Glatt, H. *Polycyclic Aromat. Compd.* **1994**, *6*, 191–198.

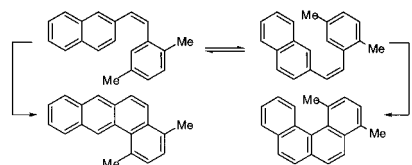
Scheme 1^a

^a Conditions: (a) 2,5-diMe-PhCH₂PPh₃⁺Cl⁻ (**6**), NaOMe, MeOH, room temperature. (b) *hν*, PhH (see discussion). (c) BBr₃, CH₂Cl₂, -78 °C to room temperature. (d) [PhSe(O)₂O], THF, reflux. (e) NaBH₄, THF-EtOH, O₂. (f) *m*-CPBA, THF, NaHCO₃.

documented. The high steric congestion resulting from introduction of the methyl group into the fjord-region (Figure 1) could destabilize the intermediate that was expected to lead to 1,4-DMBcPh and cause the reaction to follow alternative pathways; for example, 1,4-dimethylbenzo[*a*]anthracene might be produced.¹⁵ Alternatively, the photolysis might not proceed at all. On the other hand, synthesis of helicenes via a photolytic ring closure is known to be successful,^{16,17} and in an unrelated synthesis,¹⁸ we were able to incorporate a methoxy group into the fjord-region of BcPh. Additionally, a bromine atom has also been successfully incorporated into the fjord-region of BcPh.¹⁹ On the basis of these observations, and the operational simplicity of a photochemical route, we investigated the possible synthesis of 1,4-DMBcPh by this method.

The naphthylstyrene substrate **7** (Scheme 1) required for the photolysis was readily prepared as follows. Commercially available 2,5-dimethylbenzyl chloride was converted to the phosphonium salt **6**. A Wittig condensation of **6** with 2-naphthaldehyde (**4**) afforded styrene **7** as a *cis/trans* mixture (GC ratio ~1:1.5). To our delight, photolytic oxidative ring closure of **7**, with a 450-W medium-pressure Hg lamp, and a catalytic

(15) The high steric congestion caused by the fjord-region methyl group in the benzo[*c*]phenanthrene skeleton could be somewhat alleviated by ring-closure to the benzo[*a*]anthracene ring system.



Formation of the benzo[*a*]anthracene system proceeds through an intermediate in which aromaticity in all rings is disrupted and is generally regarded unfavorable. In contrast, in the intermediate leading to the benzo[*c*]phenanthrene system, one angular ring maintains aromaticity (see: Mallory, F. B.; Mallory, C. W.; Loeb, S. E. *S. Tetrahedron Lett.* **1985**, 25, 3773–3776).

(16) For a review, see: Martin, R. H. *Angew. Chem., Int. Ed. Engl.* **1974**, 13, 649–660.

(17) For some examples on the synthesis of hindered helicenes, see: Yamamoto, K.; Ikeda, T.; Kitsuki, T.; Okamoto, Y.; Chikamatsu, H.; Nakazaki, M. *J. Chem. Soc., Perkin Trans. 1* **1990**, 271–276. Liu, L.; Katz, T. J. *Tetrahedron Lett.* **1991**, 32, 6831–6834. Yang, B.; Liu, L.; Katz, T. J.; Liberko, C. A.; Miller, L. L. *J. Am. Chem. Soc.* **1991**, 113, 8993–8994. Willmore, N. D.; Liu, L.; Katz, T. J. *Angew. Chem., Int. Ed. Engl.* **1992**, 31, 1093–1095.

(18) Photochemical ring closure of 1-(2-naphthyl)-2-(3-methoxyphenyl)-ethene using catalytic I₂ produced a mixture of 3- and 1-methoxybenzo[*c*]phenanthrene. In the latter case, the oxygen resides in the fjord-region: Lakshman, M. K. unpublished observation.

(19) Plater, M. J. *J. Chem. Soc., Perkin Trans. 1* **1997**, 2903–2909.

quantity of iodine under air sparge, proceeded smoothly and afforded 1,4-DMBcPh (**3**) in 53–55% yield. Although a modification of the photochemical ring-closure method that employs stoichiometric iodine and propylene oxide is known to provide higher product yields,²⁰ the reactions cannot normally be performed with high substrate concentrations. Since **3** could be obtained in reasonable yield by the method described earlier, we did not see it necessary to apply this methodology. At this stage, we have demonstrated the effectiveness of the photochemical method for preparing 1,4-DMBcPh and have shown that the introduction of a methyl group into the fjord-region is not a deterrent to the reaction.

The next stage in the synthesis was the preparation of a suitably substituted 1,4-DMBcPh derivative, in which the substituent could be used as a handle for elaboration of the system to the oxidized metabolites. For this, a methoxy substituent is optimal, and since 6-methoxy-2-naphthaldehyde (**5**) is commercially available, it was used as the starting material (Scheme 1). A Wittig condensation of **6** with **5** afforded the methoxynaphthylstyrene **8** also as a *cis/trans* mixture (GC ratio ~1:2.3). Photochemical ring closure of **8**, as in the case of **7** proceeded smoothly and afforded 10-methoxy-1,4-dimethylbenzo[*c*]phenanthrene (**9**), albeit only in 38% yield. In an attempt to improve the yield for this step, we implemented the modified photochemical ring closure²⁰ described above (stoichiometric iodine and propylene oxide). This procedure did provide a significant although not spectacular yield improvement, and **9** was obtained in a respectable 58% yield. The next step, cleavage of the methoxy group in **9**, was effected through the use of BBr₃ in CH₂Cl₂. Phenol **10** thus obtained was subsequently oxidized to the *o*-quinone **11** with benzeneseleninic anhydride in refluxing THF. This compound was a single entity based on its ¹H NMR spectrum, which was also consistent with its structure.

Reduction of non-bay-region PAH *o*-quinones with NaBH₄ in EtOH under an oxygen atmosphere is known to produce the corresponding *trans* dihydrodiols.²¹ When this procedure was applied to **11**, the NMR spectrum of the product **12** was a 3:1 mixture of dihydrodiols. This ratio remained unchanged when the reduction was performed at 50 °C. However, the reduction was faster at the elevated temperature. Initially, we suspected that, contrary to the known reduction of *o*-quinones,²¹ **11** had undergone reduction to a mixture of *cis* and *trans* dihydrodiols. In such an event, the *cis* dihydrodiol would be separable from the *trans* isomer. However, HPLC analysis of **12** produced a single peak, as did the 9,10-diacetate and 9,10-bis-*tert*-butyldimethylsilyl ether derivatives. *Cis* dihydrodiols are also expected to form acetonides with 2,2-dimethoxypropane, but no such derivative was observed to form from **12**.

On the other hand, closer scrutiny of the ¹H NMR spectrum of **12** revealed that both dihydrodiols had a large *J*_{9,10} (~10 Hz), indicating that the hydroxyl groups in each component were in an equatorial orientation and that the carbinol protons were axial. This would not be the case for a *cis* isomer where *J*_{9,10} would be <3 Hz. Thus, convinced that the *o*-quinone had undergone the known stereoselective *trans* reduction,²¹ we began to seek less obvious explanations for the observed phenomenon.

Atropisomerism Exhibited by the Dihydrodiols of 1,4-DMBcPh. From the X-ray analysis (described below), it was obvious that introduction of the fjord-region methyl group had caused substantial (37°) out-of-plane distortion of the BcPh

(20) Liu, L.; Yang, B.; Katz, T. J.; Poindexter, M. K. *J. Org. Chem.* **1991**, 56, 3769–3775.

(21) Platt, K. L.; Oesch, F. *J. Org. Chem.* **1983**, 48, 265–268.

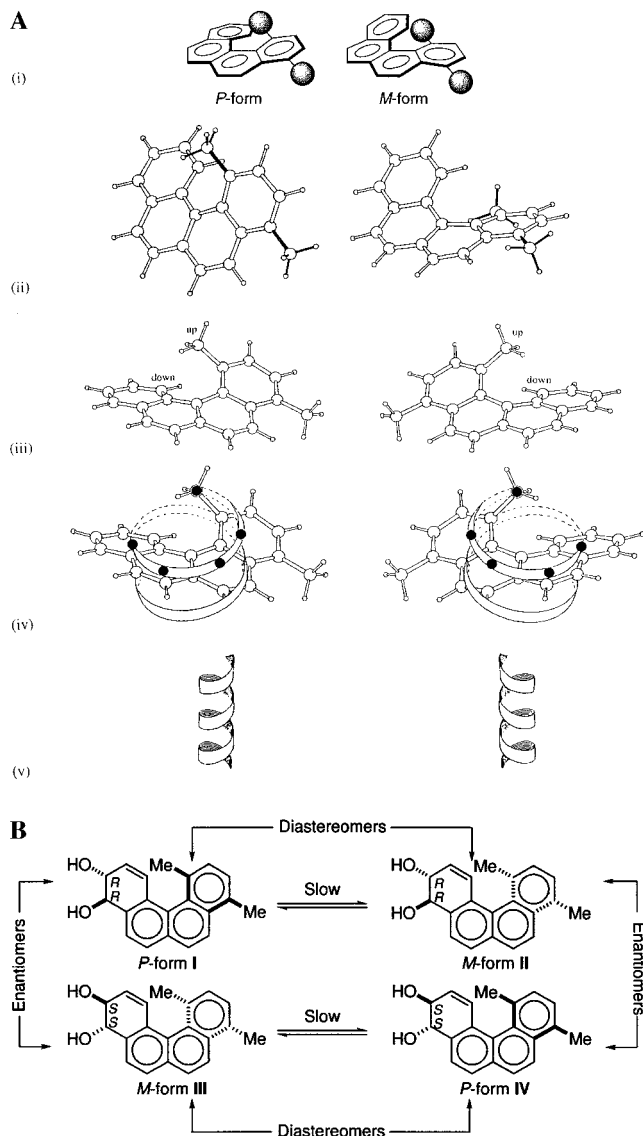


Figure 2. (A) (i) The *P*, *M* atropisomers of 1,4-dimethylbenzo[*c*]phenanthrene. (ii) View of the crystal structure of 1,4-dimethylbenzo[*c*]phenanthrene, drawn in approximately the same orientation as in (i). The two methyl groups are highlighted with filled bonds. The ring furthest from the two methyl groups is drawn in the same orientation in both the *P* and *M* forms. (iii) Views of the enantiomers of 1,4-dimethylbenzo[*c*]phenanthrene showing helicity. (iv) The same as in (iii), but with filled circles added to the centers of the rings and the helicity indicated. (v) Overall helicities of *P* and *M* forms. (B) Structures of the four dihydrodiols of 1,4-dimethylbenzo[*c*]phenanthrene and their relationships with one another.

framework. This extent of distortion causes the hydrocarbon to have helical properties so that it exists as an enantiomeric pair of *P* and *M* atropisomers (Figure 2A). Reduction of non-bay-region PAH *o*-quinones normally produces an enantiomeric pair of (*R,R*)- and (*S,S*)-*trans*-dihydrodiols.²¹ In the present case, the *o*-quinone **11**, which could exist as a pair of *P* and *M* enantiomers, upon reduction would then produce four dihydrodiols (Figure 2B). Among these the (*R,R*)-diol of the *P* helical hydrocarbon (**I**) and the (*S,S*)-diol of the *M* form (**III**) constitute a pair of enantiomers, and a similar relationship exists between the remaining two dihydrodiols (**II** and **IV**) as well. However, the enantiomeric pairs bear a diastereomeric relationship with one another. Thus, each pair of diols can produce separate NMR resonances. High steric hindrance in the fjord-region could make the *P* → *M* interconversion very slow on the NMR time scale,

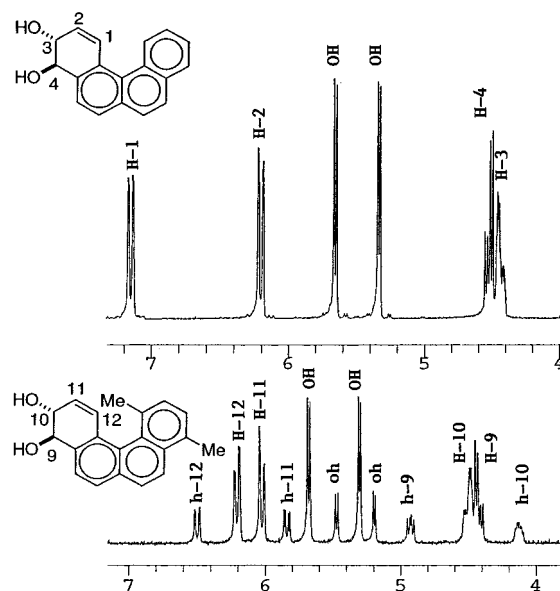


Figure 3. Partial ¹H NMR spectra (in DMSO-*d*₆) of the angular ring protons 1–4 of 3,4-dihydroxy-3,4-dihydrobenzo[*c*]phenanthrene (upper trace) and 9–12 of 9,10-dihydroxy-9,10-dihydro-1,4-dimethylbenzo[*c*]phenanthrene (lower trace). Protons of the major isomer are labeled H while those of the minor isomer are labeled h.

producing individual NMR resonances rather than averaged ones. Figure 3 shows the aliphatic resonances of BcPh and 1,4-DMBcPh dihydrodiols. The observation of one set of signals for the aliphatic protons in BcPh dihydrodiol indicates the rate of interconversion of the *P* and *M* atropisomers is fast on the NMR time scale in comparison to the 1,4-dimethyl analogue.

Assignment of Proton Resonances to the *P* and *M* Dihydrodiols of 1,4-DMBcPh. We have attempted assignment of the major and minor proton resonances to the *P* and *M* forms of dihydrodiol **12**. As can be seen from Figure 2B, the C-1 methyl and the C-10 carbinol proton are on the same face of the molecule in the (*R,R*)-*P*/(*S,S*)-*M* (**I/III**) enantiomeric pair. Whereas in the (*R,R*)-*M*/(*S,S*)-*P* (**II/IV**) pair, they are on opposite sides. Thus, evaluation of the proximity of the C-1 methyl and the C-10 carbinol proton through NOE experiments would provide clues to assigning the major and minor isomers in the NMR spectrum of the dihydrodiol. As shown in the NOESY spectrum (Figure 4), the C-1 methyl and the C-10 carbinol protons of the major isomer display a NOE cross-peak (Figure 4, shown in the box), whereas no such NOE cross-peak between these protons is seen in the minor isomer. On the basis of this, the (*R,R*)-*P*/(*S,S*)-*M* dihydrodiols (**I** and **III**) are the major diastereomeric isomers in the mixture, and the (*S,S*)-*P*/(*R,R*)-*M* dihydrodiols (**IV** and **II**) are the minor pair. Interconversion between the major and minor isomers is evident from exchanged cross-peaks in the NOESY spectrum (designated E in Figure 4). The rate of interconversion between these two sets of dihydrodiols is estimated at <50 s⁻¹.

Once a clear picture was obtained about the components of **12**, the final step was an epoxidation with *m*-CPBA. PAH dihydrodiols that have a quasi-equatorial arrangement of hydroxyl groups undergo stereoselective epoxidation with *m*-CPBA from the same side as the allylic hydroxyl group.²² Thus, epoxidation of **12** afforded a mixture of diol epoxides **13** whose ratio was consistent with the composition of **12**.

Table 1 shows the angles between the planes of the four aromatic rings (labeled A–D) in BcPh and 1,4-DMBcPh; thus

(22) Yagi, H.; Thakker, D. R.; Hernandez, O.; Koreeda, M.; Jerina, D. *M. J. Am. Chem. Soc.* **1977**, *99*, 1604–1611.

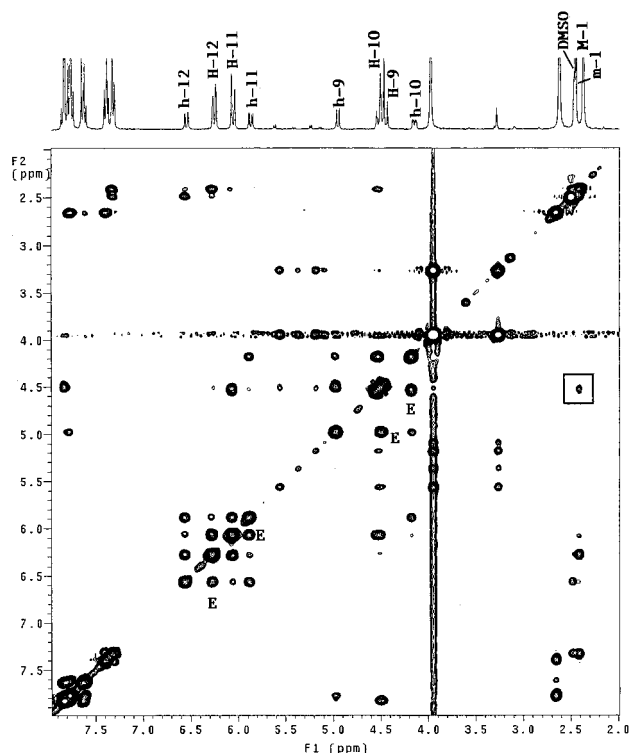


Figure 4. NOESY (2-s mixing time) spectrum of 9,10-dihydroxy-9,10-dihydro-1,4-dimethylbenzo[*c*]phenanthrene (in DMSO-*d*₆, 40 °C) recorded at 300 MHz. The close proximity between the 1-methyl and the C-10 carbinol protons in the major isomer is evident from the presence of the through space NOE cross-peak (shown in the box). Exchanged cross-peaks resulting from interconversion between C-9 to C-12 protons in the major and minor isomers are shown as E. Proton assignment for the major (H-9 to H-12, M-1) and minor (h-9 to h-12, m-1) isomers are shown in the 1-D spectrum (top).

Table 1. Angles between the Planes of the Aromatic Rings in BcPh and 1,4-DMBcPh

Angle Between		
A, B	11.66°	10.26°
A, C	24.70°	18.12°
A, D	36.65°	26.68°
B, C	13.07°	7.87°
B, D	25.02°	16.55°
C, D	12.45°	8.83°

a direct comparison is possible. As can be seen from Table 1, the angles between the A/B planes are not substantially different in the two compounds. However, a remarkable distortion of the B/C naphthalene unit is seen in 1,4-DMBcPh compared to BcPh. Not unexpectedly, this compound also shows a substantial distortion of the C/D ring planes. The net result is that the A/C plane angle of 1,4-DMBcPh is nearly the same as the A/D angle of BcPh. The angle between the A/D planes is a measure of overall distortion of the molecules from planarity; BcPh is distorted by 26.7° whereas, in 1,4-DMBcPh this distortion is increased by 10–37°.

Activation of PAHs in MCF-7 Cells. The ability of human cells to activate PAHs to DNA binding-intermediates was evaluated by treating MCF-7 human mammary carcinoma cells with BaP, BcPh, and 1,4-DMBcPh for 24 h, followed by isolation of the DNA and analysis by ³²P postlabeling as well

Table 2. PAH–DNA Adduct Concentration Results (pmol of Adduct/mg of DNA) from the Activation and Binding of BaP, BcPh, and 1,4-DMBcPh, as Well as the BcPh and 1,4-DMBcPh Dihydrodiols Using MCF-7 Cells^a

	BaP (4 μM)	BcPh (5 μM)	1,4-DMBcPh (5 μM)	BcPh dihydrodiol (1 μM)	1,4-DMBcPh dihydrodiol (1 μM)
average	65.2	3.1*	1.1*	13.2†	1.2†
std dev	5.3	1.6	0.5	1.9	0.6

^a MCF-7 cells treated with either 4 μM BaP, 5 μM BcPh, 5 μM 1,4-DMBcPh, 1 μM BcPh dihydrodiol, or 1 μM 1,4-DMBcPh dihydrodiol and harvested after 24 h. Isolated DNA were postlabeled in triplicate (average value ± standard deviation). Using a two-tailed unpaired *t*-test, * indicates values that are not significantly different, *p* = 0.1077 and † indicates values that are significantly different, *p* < 0.0005.

as HPLC. Similar treatment was also performed with the dihydrodiol of 1,4-DMBcPh (12) and the corresponding BcPh dihydrodiol. The results are shown in Table 2. These data reveal an almost 3-fold higher level of DNA binding with BcPh as compared to 1,4-DMBcPh. In contrast to the planar BaP, BcPh is only poorly converted to DNA-damaging species. The trend therefore seems to imply that increasing the nonplanarity of a PAH lowers its ability to undergo metabolism to reactive forms that produce DNA-damaging adducts. However, the dihydrodiol derivatives of BcPh and 1,4-DMBcPh revealed a highly significant 11-fold difference in DNA adduct formation. When considering the metabolic activation of PAHs, the first step is the formation of the arene oxide that is then hydrolyzed to the dihydrodiol and further oxidized to the diol epoxide. Although there is a 3-fold difference in the activation of the parent PAHs that may be dependent on the extent of PAH nonplanarity, activation of the dihydrodiols occurs at the region where the influence of distortion is maximal.

Conclusions

We have prepared, for the first time, the most nonplanar oxidized derivatives among the dihydrodiol and diol epoxide metabolites of PAHs. In this process, we have shown that the high steric congestion resulting from introduction of the methyl group into the fjord-region is accommodated by a twist of the PAH. Therefore, in contrast to dihydrodiols of BcPh and 1,4-difluoro BcPh,²³ which show average signals on the NMR time scale, 1,4-DMBcPh dihydrodiol exists as slowly interconverting helical isomers. This raises an important question: is it possible that in highly hindered diol epoxide–DNA lesions of nonplanar PAHs, the helical properties of the PAH residue could also be factor that needs consideration in the assessment of structure–biology correlations? On the basis of the comparative metabolic activation and DNA binding studies we have demonstrated that 1,4-DMBcPh is as poorly metabolized to DNA binding intermediates as BcPh. However, there is a significant difference in the levels of DNA binding of the dihydrodiol compounds, possibly as a result of distortions in a region with maximal impact. When considered in light of the metabolic activation of the planar PAH BaP, it appears that nonplanar BcPh and its dimethyl analogue may be poorer substrates for P450 1B1, which is constitutively present at high levels in MCF-7 cells, thereby resulting in poor metabolic activation to DNA alkylating metabolites. However, in 1,4-DMBcPh, the metabolic activation could also be affected by the presence of the two methyl groups in one of the angular rings. Despite the lowered activation, the metabolites of nonplanar PAHs are often found to be potent carcinogens.

(23) Lakshman, M. K.; Chaturvedi, S.; Bae, S. Y.; Hahn, H.-G.; Mah, H., unpublished data.

Experimental Section

Photochemical ring closures were performed with a Hanovia photoreactor using a 450-W medium-pressure Hg lamp and a Pyrex filter. The course of the photochemical reactions was monitored by GC: capillary column SBP-20, 20% diphenyl-80% dimethylsiloxane (0.5-m film, 0.53 mm i.d. \times 30 m). The initial column temperature was 150 °C, which was ramped at a rate of 20 °C/min to reach a final column temperature of 295 °C; the injector was maintained at 200 °C and the detector at 250 °C. Where required, anhydrous solvents were purchased and used without further purification. For the epoxidation reactions, commercially available *m*-CPBA (57–86%) was purified as described²⁴ using commercially available pH 7.4 buffer. Column chromatography was performed on 230–400-mesh silica gel. NMR spectra were recorded in CDCl₃ unless otherwise noted. Chemical shifts (δ) are in ppm and coupling constants (*J*) are in hertz. In cases where two isomers are seen in the NMR spectrum, specific signal assignments are made as follows: maj isomer (for major isomer) and min isomer (for minor isomer). All 1,4-DMBCPh compounds are numbered so that the fjord-region, methyl-bearing carbon is C-1. Nuclease P1, *Crotalus atrox* venom phosphodiesterase (type VII), prostatic acid phosphatase, potato apyrase (grade VII), and proteinase K were obtained from Sigma Chemical Co. Redistilled phenol, RNase, and RNase T1 were purchased from Boehringer-Mannheim Co. Cloned T4 polynucleotide kinase was obtained from United States Biochemical Corp. [³²P]ATP was purchased from NEN-Dupont. BaP was obtained from Chemsyn Science Laboratories. BcPh, and (\pm)-BcPh 3,4-dihydrodiol (BcPh diol) were prepared through published procedures.

2,5-Dimethylbenzyltriphenylphosphonium Chloride (6). To a stirred solution of 2,5-dimethylbenzyl chloride (1 g, 6.47 mmol) in toluene (10 mL) was added triphenylphosphine (1.86 g, 7.09 mmol). The mixture was heated at reflux overnight. The precipitated solid was filtered and washed with hexane to yield phosphonium salt **6** as a colorless powder (2.07 g, 76%). This was used for subsequent reactions without further purification.

1-(2,5-Dimethylphenyl)-2-(2-naphthyl)ethene (7). To a solution of **6** (2.07 g, 4.98 mmol) in MeOH (15 mL) was added a 25% (w/v) solution of NaOMe in MeOH (2.15 mL, 9.95 mmol NaOMe). A curdy white precipitate was seen to form, the mixture was allowed to stir at room temperature for 45 min, and then to the mixture were added 2-naphthaldehyde (**4**) (0.699 g, 4.48 mmol) followed by MeOH (5 mL). After the reaction was allowed to proceed at room temperature overnight, the mixture was diluted with Et₂O and washed with H₂O. The organic layer was dried (Na₂SO₄) and evaporated. The product was impregnated onto silica gel, and the mixture was loaded onto a dry-packed silica column. Elution with 20% PhH in hexane afforded **7** as a colorless powder, ~1:1.5 mixture of cis/trans olefins (1.103 g, 95%): *R*_f (10% PhH in hexane) = 0.56 and 0.60. Crystallization of an analytical sample from MeOH provided an alkene mixture that was enriched in the more polar isomer: mp 114–116 °C; ¹H NMR 7.87–7.65, 7.58–7.40 (m, Ar), 7.27 (s), 7.22–7.00 (m, Ar), 6.74 (AB_{quartet}, 2H_{1,2}, *J* = 12.1), 2.44 (s, 3H, Me_{maj isomer}), 2.39 (s, 3H, Me_{maj isomer}), 2.24 (s, 3H, Me_{min isomer}), 2.18 (s, 3H, Me_{min isomer}); HRMS calcd for C₂₀H₁₉ (M⁺ + 1) 259.1487, found 259.1475. Anal. Calcd for C₂₀H₁₈: C, 92.98; H, 7.02. Found: C, 92.62; H, 7.11.

1,4-Dimethylbenzo[*c*]phenanthrene (3). The photochemical ring closure was performed on two 1.2-g aliquots of **7** as follows. Alkene **7** (1.2 g, 4.65 mmol) was dissolved in PhH (1 L). A catalytic quantity of I₂ was added and the mixture was photolyzed, while a sparge of air was maintained through the mixture for the entire duration of the reaction. The reaction could be readily monitored by GC (*t*_{R(7)} = 5.32 and 6.60 min; *t*_{R(3)} = 6.80 min). Upon completion of the reaction (usually within 6 h), the mixture was evaporated to dryness. The combined products from the two runs were redissolved in CH₂Cl₂ and washed with 5% aqueous Na₂S₂O₃ (100 mL). The organic layer was dried (Na₂SO₄) and evaporated. The product was impregnated onto silica gel, and the mixture was loaded onto a dry-packed silica column. Elution with 20% PhH in hexane afforded 1,4-DMBCPh as a colorless solid which upon crystallization from MeOH provided pure **3** as

colorless crystals (1.33 g, 55%): *R*_f (10% PhH in hexane) = 0.57; mp (from MeOH) 123–124 °C; ¹H NMR 8.08–7.78 (m, 6H_{Ar}), 7.59–7.53 (m, 2H_{Ar}), 7.45 (AB_{quartet}, 2H_{2,3}, *J* = 7.7), 2.82 (3H, Me), 2.37 (s, 3H, Me); HRMS calcd for C₂₀H₁₇ (M⁺ + 1) 257.1330, found 257.1328. Anal. Calcd for C₂₀H₁₆: C, 93.71; H, 6.29. Found: C, 93.23; H, 6.41.

1-(2,5-Dimethylphenyl)-2-(6-methoxy-2-naphthyl)ethene (8). To a stirred solution of **6** (9.53 g, 22.9 mmol) in MeOH (200 mL) was added a 25% (w/v) solution of NaOMe in MeOH (9.9 mL, 45.8 mmol). After the mixture was allowed to stir at room temperature for 1.5 h, 6-methoxy-2-naphthaldehyde (**5**) (3.88 g, 20.8 mmol) was added, and the stirring was continued for 36 h. The mixture was diluted with CH₂-Cl₂ and washed with H₂O. Evaporation of the organic layer after drying (Na₂SO₄) afforded the crude alkene mixture which was impregnated onto silica gel. This compound/silica mixture was loaded onto a dry-packed silica column and eluted with 30% PhH in hexane. The product, a colorless fluffy powder, was a ~1:2.3 mixture of cis/trans alkenes **8** (5.88 g, 98%): *R*_f (30% PhH in hexane) = 0.36 and 0.41; mp moistens at 87–90 °C and completely melts at 110–112 °C; ¹H NMR 7.80–7.73, 7.59–7.37, 7.17–7.03 (m, Ar), 6.69 (AB_{quartet}, 2H_{1,2}, *J* = 12.2), 3.94 (s, 3H, OMe_{maj isomer}), 3.90 (s, 3H, OMe_{min isomer}), 2.43 (s, 3H, Me_{maj isomer}), 2.38 (s, 3H, Me_{maj isomer}), 2.23 (s, 3H, Me_{min isomer}), 2.19 (s, 3H, Me_{min isomer}); HRMS calcd for C₂₁H₂₁O (M⁺ + 1) 289.1592, found 289.1609. Anal. Calcd for C₂₁H₂₀O: C, 87.46; H, 6.99. Found: C, 87.24; H, 7.15.

10-Methoxy-1,4-dimethylbenzo[*c*]phenanthrene (9). The preparation of this compound by photolytic ring closure was performed using either catalytic I₂ or stoichiometric I₂ and propylene oxide. Both methods are described below, however, the second method afforded better yields.

Method 1: Using Catalytic I₂ and Air. The alkene (3.48 g) was photolyzed in two equal batches. To a solution of the alkene **8** (1.74 g, 6.08 mmol) in PhH (1 L) was added I₂ (25 mg). This mixture was subjected to photolysis while a sparge of air was maintained through the mixture for the entire course of the reaction. The reaction was complete within 6 h. The course of the reaction could be readily monitored by GC (*t*_{R(8)} = 6.25 and 7.46 min; *t*_{R(9)} = 7.63 min). The mixture was evaporated to dryness. The products from the two runs were redissolved in CH₂Cl₂, and washed with 2% aqueous Na₂S₂O₃ (100 mL). The organic layer was dried (Na₂SO₄) and evaporated. The product was impregnated onto silica gel, and the mixture was loaded onto a dry-packed silica column. Elution with 30% PhH in hexane afforded **9** as a colorless fluffy powder (1.33 g, 38%).

Method 2: Using Stoichiometric I₂ and Propylene Oxide. This procedure was performed on 2.28 g of **8** in four batches according to the procedure described below. Argon was bubbled for 15 min through a solution of the alkene **8** (0.6 g, 2.1 mmol) and I₂ (0.53 g, 2.1 mmol) in PhH (900 mL) and propylene oxide (100 mL). The mixture was then photolyzed as described previously and was judged to be complete after 23 h. The clear yellow solution was evaporated to dryness. The products from the four batches were combined and subjected to the Na₂S₂O₃ wash as well as chromatography as described in method 1. The product obtained was triturated with MeOH to afford **9** as a colorless powder (1.03 g, 58%).

An analytical sample was recrystallized from MeOH to provide **9** as colorless microcrystals: *R*_f (30% PhH in hexane) = 0.26; mp (from MeOH) 187–188 °C; ¹H NMR 7.96 (d, 1H_{Ar}, *J* = 8.8), 7.93 (d, 1H_{Ar}, *J* = 9.2), 7.85 (app s, 2H_{Ar}), 7.73 (d, 1H_{Ar}, *J* = 8.5), 7.41 (AB_{quartet}, 2H_{2,3}, *J* = 7.7), 7.32 (d, 1H₉, *J* = 2.6), 7.20 (dd, 1H₁₁, *J* = 2.6, 9.2), 4.00 (s, 3H, OMe), 2.80 (s, 3H, Me), 2.36 (s, 3H, Me); HRMS calcd for C₂₁H₁₈O (M⁺) 286.1358, found 286.1365. Anal. Calcd for C₂₁H₁₈O: C, 88.08; H, 6.34. Found: C, 87.21; H, 6.45.

10-Hydroxy-1,4-dimethylbenzo[*c*]phenanthrene (10). BB₃ (2.13 mL of a 1M solution in CH₂Cl₂, 2.1 mmol) was added to a stirred solution of **9** (0.3 g, 1.06 mmol) in CH₂Cl₂ (25 mL) at –78 °C. The mixture was allowed to warm to room temperature and stirred for 4 h. Nitrogen was sparged through the solution, and the mixture was washed with H₂O to neutrality. Drying of the organic layer (Na₂SO₄) and evaporation afforded a foam. Crystallization of this material from CH₂-Cl₂/hexane yielded **10** as light pinkish fine needles (0.27 g, 94%): *R*_f (20% THF in hexane) = 0.40; mp (from CH₂Cl₂-hexane) 138–139 °C; ¹H NMR 7.99 (d, 1H_{Ar}, *J* = 8.7), 7.94 (d, 1H_{Ar}, *J* = 9.0), 7.82

(24) Armarego, W. L. F.; Perrin, D. D. *Purification of Laboratory Chemicals*, 4th ed.; Butterworth Hinemann: Boston, 1997; p 145.

(AB_{quartet}, 2H_{Ar}, $J = 8.4$), 7.75 (d, 1H_{Ar}, $J = 8.7$), 7.41 (AB_{quartet}, 2H_{2,3}, $J = 7.5$), 7.31 (d, 1H₉, $J = 2.7$), 7.14 (dd, 1H₁₁, $J = 2.7, 9.0$), 5.18 (s, 1H_{OH}), 2.80 (s, 3H, Me), 2.36 (s, 3H, Me); HRMS calcd for C₂₀H₁₆O: (M⁺) 272.1201, found 272.1228.

1,4-Dimethylbenzo[*c*]phenanthren-9,10-dione (11). A mixture of benzeneseleninic anhydride (2.3 g, 6.25 mmol) and the phenol **10** (0.5 g, 1.8 mmol) were heated at reflux in anhydrous THF (100 mL) for 2 h, under an argon atmosphere. The mixture was cooled, diluted with EtOAc, and washed with H₂O. The organic layer was separated, dried (Na₂SO₄), and evaporated. The product was combined with that from a second reaction on 1.46 g of **10** and subjected to flash chromatography using CH₂Cl₂ to afford quinone **11** as a dark red powder (1.94 g, 94%): R_f (20% THF in hexane) = 0.45; recrystallization of an analytical sample from EtOAc afforded dark red flakes, mp 193–194 °C; ¹H NMR 8.25 (d, 1H_{Ar}, $J = 8.1$), 7.97 (d, 1H_{Ar}, $J = 9.2$), 7.89 (d, 1H_{Ar}, $J = 8.1$), 7.70 (d, 1H₁₂, $J = 10.3$), 7.56 (d, 1H_{Ar}, $J = 9.2$), 7.44 (AB_{quartet}, 2H_{2,3}, $J = 7.7$), 6.38 (d, 1H₁₁, $J = 10.3$), 2.74 (s, 3H, Me), 2.63 (s, 3H, Me); HRMS calcd for C₂₀H₁₅O₂ (M⁺ + 1) 287.1072, found 287.1096.

(±)-trans-9,10-Dihydroxy-9,10-dihydro-1,4-dimethylbenzo[*c*]phenanthrene (12). Quinone **11** (0.5 g, 1.75 mmol) was dissolved in THF (30 mL) and EtOH (200 mL) was added. The mixture was heated at 50 °C and sparged with O₂. NaBH₄ (0.66 mg, 17.5 mmol) was added portionwise, and after 2 h, another aliquot of NaBH₄ (0.66 mg, 17.5 mmol) was added portionwise. After a total reaction time of 4 h, the mixture was concentrated to a smaller volume. Addition of H₂O caused precipitation of a colorless solid which was filtered and washed with H₂O. The crude dihydrodiol **12** (0.5 g) was recrystallized from THF to yield two crops (0.22 and 0.08 g, respectively, total of 60%) of pure diol **12**: R_f (THF/hexanes/Et₃N 1:1:0.1) = 0.43; mp (from THF) 204–205 °C; ¹H NMR (DMSO-*d*₆) 7.82–7.69, 7.61–7.56, 7.37–7.27 (m, 6H_{Ar} maj and min isomers), 6.51 (dd, 1H₁₂ min isomer, $J = 1.0; 10.0$), 6.21 (dd, 1H₁₂ maj isomer, $J = 2.0; 10.1$), 6.03 (dd, 1H₁₁ maj isomer, $J = 1.7; 10.0$), 5.84 (dd, 1H₁₁ min isomer, $J = 3.4; 10.0$), 5.68 (d, 1H_{OH} maj isomer, $J = 5.7$), 5.48 (d, 1H_{OH} min isomer, $J = 5.5$), 5.31 (d, 1H_{OH} maj isomer, $J = 4.7$), 5.20 (d, 1H_{OH} min isomer, $J = 4.9$), 4.88 (dd, 1H₉ min isomer, $J = 5.5; 8.8$), 4.53–4.50 (m, 1H₁₀ maj isomer), 4.45–4.40 (dd, 1H₉ maj isomer, $J = 5.7, 11.5$), 4.13 (m, 1H₁₀ min isomer), 2.63 (s, 3H, 4-Me maj and min isomer), 2.46 (s, 3H, 1-Me min isomer), 2.30 (s, 3H, 1-Me maj isomer). Collapse of the following signals was observed upon exchange with MeOH-*d*₄: 4.88 (d, 1H₉ min isomer, $J = 8.8$), 4.53–4.50 (dd, 1H₁₀ maj isomer, $J = 2.1; 11.3$), 4.45–4.40 (d, 1H₉ maj isomer, $J = 11.3$), 4.14–4.10 (ddd, 1H₁₀ min isomer, $J = 1.1; 3.6; 8.8$); HRMS calcd for C₂₀H₁₉O₂ (M⁺ + 1) 291.1385, found 291.1407.

(±)-11α,12α-Epoxy-9β,10α-dihydroxy-9,10-dihydro-1,4-dimethylbenzo[*c*]phenanthrene (13). Solid NaHCO₃ (200 mg) was added to a solution of dihydrodiol **12** (0.1 g, 0.35 mmol) in anhydrous THF (10 mL), the mixture was flushed with argon and cooled to –78 °C. Purified *m*-CPBA²⁴ (0.2 g, 1.16 mmol) was added, and the mixture was allowed to stir at ambient for 1 h. The mixture was then diluted with EtOAc and washed sequentially with ice-cold 10% aq KOH (4 × 5 mL) and water followed by brine. The organic layer was dried (K₂CO₃) and evaporated to provide the diol epoxide **13** as a colorless powder (0.083 g, 78%). A portion of the product was recrystallized from THF (1 mL) and Et₃N (50 μL) and used for recording the NMR and mass spectra: R_f (THF/hexanes/Et₃N 1:1:0.1) = 0.52; mp (from THF/Et₃N) 192–193 °C; ¹H NMR (THF-*d*₆), exchanged with MeOH-*d*₄ 7.96–7.22 (m, 6H_{Ar} maj and min isomers), 4.96 (d, 1H₉ maj isomer, $J = 8.8$), 4.52 (d, 1H₉ min isomer, $J = 8.7$), 4.45 (d, 1H₁₂ min isomer, $J = 4.2$), 4.15 (d, 1H₁₂ maj isomer, $J = 4.4$), 4.07 (d, 1H₁₀ min isomer, $J = 8.7$), 3.94 (d, 1H₁₁ min isomer, $J = 4.2$), 3.38 (m, 2H_{10,11} maj isomer), 2.77 (s, 3H, Me maj isomer), 2.70 (s, 3H, Me min isomer), 2.68 (s, 3H, Me maj isomer), 2.61 (s, 3H, Me min isomer). The hydroxyl protons appear at 4.96 maj isomer (overlaps with H₉ maj isomer), 4.87 min isomer (d, $J = 6.3$), 4.80 min isomer (d, $J = 5.2$), 4.68 maj isomer (d, $J = 5.5$); HRMS calcd for C₂₀H₁₈O₃ 306.1256, found 306.1245.

Comparative X-ray Analyses of BcPh and 1,4-DMBcPh. X-ray diffraction data were measured at 120(2) K in three different crystal orientations employing a θ offset of 30°. They were measured as frames using oscillations of 0.20° for 15 s per frame at a crystal-to-detector distance of 50 mm on an Enraf-Nonius FAST area detector diffractometer using molybdenum X-radiation [λ Mo K α = 0.710 73 Å] and

a graphite monochromator. The resulting diffraction data were processed to give values of F^2 by use of the program MADNES.²⁵ They were then merged using the program XSCALE.²⁶ The unit cell dimensions and space groups for each compound were determined from measurements on 250 Bragg reflections that had θ angles ranging from 10 to 18° and intensities $I > 25\sigma(I)$; programs MADNES²⁵ and ABSURD²⁷ were used. The crystal-to-detector distance was previously calibrated using a crystal of basic beryllium acetate, which is cubic with $a = 15.735$.

The crystal structure of 1,4-DMBcPh was determined by use of the structure solution package MULTAN88²⁸ while that of BcPh had been previously reported at room temperature^{29,30} but was remeasured here at low temperatures so that geometric data on both structures were measured under the same experimental conditions. The resulting structures were refined using the program ICRFMLS,^{31,32} modified to refine on F^2 . Hydrogen atoms were located in an $F_o - F_c$ electron density map and agreed with calculated positions. Refinement was anisotropic for all non-hydrogen atoms and isotropic for hydrogen atoms. The quantity minimized in the least-squares refinement was $\Sigma \omega(F_o^2 - F_c^2)$ and the weighting scheme used was $\omega = 1/[\sigma^2(F_o^2)]$. Scattering factors employed were those published in *International Tables for X-ray Crystallography*.³³

(1) Benzoc[*c*]phenanthrene. The crystal used for study was a colorless lath 0.2 × 0.10 × 0.04 mm. It was orthorhombic with unit cell dimensions $a = 14.451(4)$, $b = 13.884(1)$, $c = 5.800(1)$ Å, in the space group $P2_12_12_1$. A total of 6622 Bragg reflections were measured, of which 2150 were with $R_{\text{merge}}(I) = 0.070$. The symmetry-equivalent reflections were then combined to yield 1253 unique data with $R_{\text{sym}}(I) = 0.096$. The maximum value of $\sin\theta/\lambda$ for these data is 0.603 ($\theta = 25.4^\circ$). The agreement between calculated and observed structure factors is good with $R_1 = 0.061$ and $wR_1 = 0.038$ with respect to F for all 840 data. The agreement with respect to F^2 (the basis of this structure refinement) was $R_2 = 0.066$ and $wR_2 = 0.0765$. The goodness of fit is 1.052. The minimum and maximum electron densities in the final difference Fourier map are –0.191 and +0.189 e/Å³, respectively.

(2) 1,4-Dimethylbenzo[*c*]phenanthrene. The crystal used for study was a colorless trapezoid 0.25 × 0.15 × 0.04 mm in dimensions. It was monoclinic with unit cell dimensions $a = 8.812(3)$, $b = 8.266(2)$, $c = 9.497(8)$ Å and $\beta = 103.47(4)^\circ$, space group $P2_1$. A total of 7022 Bragg reflections were measured, of which 2910 were redundant with $R_{\text{merge}}(I) = 0.048$. The symmetry-equivalent reflections were then combined to yield 1784 unique data with $R_{\text{sym}}(I) = 0.061$. The maximum value of $\sin\theta/\lambda$ for these data is 0.676/Å ($\theta = 28.7^\circ$). The agreement between calculated and observed structure factors is good, with $R_1 = 0.066$ and $wR_1 = 0.0679$ with respect to F for all 1530 data. The agreement with respect to F^2 (the basis of the structure refinement) was $R_2 = 0.0944$ and $wR_2 = 0.1268$. The goodness of fit is 2.556. The minimum and maximum electron densities in the final difference Fourier map are –0.416 and +0.385 e/Å³, respectively.

The extent of distortion of the aromatic ring system of BcPh is shown in Table 1 by the angles between the planes through each aromatic system. The overcrowding in the fjord-regions, as a result of nonbonded

(25) Pflugrath, J.; Messerschmidt, A. MADNES. Munich Area Detector (New EEC) System, version EEC 11/09/89, with enhancements by Enraf-Nonius Corp., Delft, The Netherlands, 1989.

(26) Kabsch, W. *J. Appl. Crystallogr.* **1988**, *21*, 916–924.

(27) Karaulov, C. ABSURD. Program to aid in processing data from MADNES, as modified for space group determination, 1991.

(28) Debaerdemaeker, Y.; Germain, G.; Main, P.; Refaai, L. S.; Tate, C.; Woolfson, M. M. MULTAN88. Computer programs for the automatic solution of crystal structures from X-ray diffraction data. University of York, U.K., 1988.

(29) Hirshfeld, F. L.; Sandler, S.; Schmidt, G. M. *J. Chem. Soc.* **1963**, 2108–2125.

(30) Hirshfeld, F. L. *J. Chem. Soc.* **1963**, 2126–2135.

(31) Gantzel, P. K.; Sparks, R. A.; Long, R. E.; Trueblood, K. N. UCLALS4, Program in Fortran IV, 1969.

(32) Carrell, H. L. ICRFMLS, modification of UCLALS4. Program from The Institute for Cancer Research, Fox Chase Cancer Center, Philadelphia, PA, 1975.

(33) Ibers, J. A.; Hamilton, W. C., Eds. *International Tables for X-ray Crystallography*; Kynoch Press: Birmingham, England (present distributor Kluwer Academic Publishers: Dordrecht, Germany), 1974; Vol. IV.

H···H repulsions, causes the angle between A and D rings in BcPh to be 26.7°, and this is increased a further 10° when the hydrogen atom in position 1 is replaced by a more bulky methyl group in 1,4-DMBcPh.

Formation of a fjord-region diol epoxide, involving the conversion of ring A to a partially saturated ring with an additional epoxide oxygen atom attached, will greatly increase the strain in the ring. This was shown for the bay-region diol epoxide of 5,6-dimethylchrysene in which the bay-region methyl group forces the epoxide group well out of the plane of the aromatic system. The overcrowding in a fjord-region diol epoxide of 1,4-DMBcPh would be expected to be more extensive and consequent tension on bonds might affect the electron flow and thereby the molecular reactivity.

Treatment of Cell Cultures with the PAHs. The human mammary carcinoma cell line, MCF-7, was grown in 75-cm² flasks with Dulbecco's Modified Eagle Medium (D-MEM) (Gibco BRL, Grand Island, NY) and F-12 Nutrient Mixture (Gibco BRL, Grand Island, NY) in a 1:1 ratio supplemented with 10% FBS (Intergen, Purchase, NY) and containing 15 mM HEPES buffer and antibiotics (200 units/mL penicillin, 200 µg/mL streptomycin, and 25 µg/mL ampicillin) at 37 °C with 5% CO₂. Cultures in which cells covered ~90% of the surface of the flask were refed with fresh medium and 10% FBS 24 h prior to treatment. Cells were treated with 4 µM BaP, 5 µM BcPh, or 5 µM 1,4-DMBcPh in 0.1% DMSO (final concentration) for 24 h. The cells were harvested by trypsinization with 0.05% trypsin-EDTA (0.14 M NaCl, 3 mM KCl, 0.1 M Na₂HPO₄, 1.5 mM KH₂PO₄, 0.5 mM EDTA), and resulting pellets stored at -80 °C. DNA was isolated by homogenizing with 20 strokes in a Dounce homogenizer in 10 mM Tris, 1 mM EDTA containing 1% SDS, pH 8.0 and incubated with RNase (50 units/mL) and RNase T1 (1000 units/mL) for 1 h at 37 °C. This was followed by incubation with proteinase K (500 µg/mL) for 1 h at 37 °C. The DNA was extracted with phenol/chloroform/isoamyl alcohol (25:24:1) and precipitated with 1/10 volume of 5 M NaCl and 2 volumes of cold 100% ethanol. The DNA was dissolved in H₂O and quantitated on the basis of UV absorbance at 260 nm (1 AU = 50 µg of DNA).

³³P-Postlabeling of DNA Adducts. After reducing the sample volume to 5 µL with a Speed-Vac, Ten micrograms of the cellular DNA samples and of the BaP diol epoxide standards were digested with nuclease P1 (55 munits/µL) and prostatic acid phosphatase (32 munits/µL) in a total volume of 11 µL of nuclease P1 buffer (0.1 M sodium acetate, 3 mM ZnCl₂, pH 5.2) at 37 °C for 45 min. After again reducing the sample volume to 5 µL with a Speed-Vac, the digested DNA was labeled with [γ -³³P]ATP (4 µCi/µL, sp act. 2000 Ci/mmol) and T4 polynucleotide kinase (1.4 units/µL) in a total volume of 12.6

µL of kinase buffer (80 mM Tris, 16 mM MgCl₂, 16 mM DTT, 1.3 mM spermidine, pH 9.6) at 37 °C for 1 h. The labeled adducted dinucleotides were digested to mononucleotides with snake venom phosphodiesterase (0.8 munits/µL). Unused [γ -³³P]ATP was hydrolyzed with potato apyrase (5.3 munits/µL) in a total volume of 19.6 µL at 37 °C for 1 h. The labeled, adducted nucleotides were separated from other digestion products by Sep-Pak C₁₈ column chromatography as described previously.³⁴

Reversed-Phase HPLC Analysis of ³³P-Postlabeled PAH-DNA Adducts. The PAH-DNA adducts were analyzed by reversed-phase HPLC utilizing a 5-µm Ultrasphere C₁₈ column (4.6 mm × 25 cm) and an on-line radioisotope flow detector. The BcPh-DNA adducts were resolved by elution at 1 mL/min with 50 mM ammonium phosphate and 20 mM tetrabutylammonium phosphate, pH 5.5 (solvent A) and 50:50 (v/v) acetonitrile/methanol (solvent B). The elution gradients were as follows: 37–38% solvent B over 20 min, 38–40% solvent B over 20 min, 40–43% solvent B over 20 min, 43–49% solvent B over 20 min, 49–55% solvent B over 10 min, and isocratic elution at 55% solvent B for 20 min. The BaP-DNA adducts were resolved by elution at 1 mL/min with 100 mM ammonium phosphate, pH 5.5 (solvent A) and 100% methanol (solvent B). The elution gradient was as follows: 44–60% solvent B over 40 min.

Acknowledgment. This article is dedicated to Dr. Anthony Dipple (February 1940–May 1999), a pioneer in the area of chemical carcinogenesis, a mentor and a friend. The work was partially supported by NCI Contract NO1-CB-61004 (ChemSyn Science Laboratories) and NSF Grant OSR 9452892 to M.K.L. J.P.G., A.K.K., and H.L.C. were supported by NIH Grant CA-10925. The DNA adduct studies in MCF-7 cells were supported by NCI Grant CA 40228 to W.M.B. We thank Dr. Kurt Krause of Smith-Kline-Beecham for allowing us to collect a set of X-ray diffraction data in his laboratory. The contents of this paper are solely the responsibility of the authors and do not necessarily represent the official views of the National Cancer Institute.

Supporting Information Available: Atomic coordinates of 1,4-DMBcPh and BcPh (PDF). This material is available free of charge via the Internet at <http://pubs.acs.org>.

JA002072W

(34) Lau, H. H. S.; Baird, W. M. *Carcinogenesis* **1994**, *15*, 907–915.